not the differentially methylated DNA regions or antisense transcripts, marks the imprinting status of *IGF2R* in human and mouse. Hum. Mol. Genet. 13:2233–2245.

36. **Wang, J., J. Mager, Y. Chen, E. Schneider, J. C. Cross, A. Nagy, and T. Magnuson.** 2001. Imprinted X inactivation maintained by a mouse Polycomb group gene. Nat. Genet. **28**:371–375.
37. **Wang, Y., K. Joh, S. Masuko, H. Yatsuki, H. Soejima, A. Nabetani, C. V. Beechey, S. Okinami, and T. Mukai.** 2004. The mouse *Murr1* gene is imprinted in the adult brain, presumably due to transcriptional interference by the antisense-oriented *U2af1-rs1* gene. Mol. Cell. Biol. **124**:270–279.
38. **Yamasaki, K., K. Joh, T. Ohta, H. Masuzaki, T. Ishimaru, T. Mukai, N. Niikawa, M. Ogawa, J. Wagstaff, and T. Kishino.** 2003. Neurons but not glial cells show reciprocal imprinting of sense and antisense transcripts of *Ube3a*. Hum. Mol. Genet. **12**:837–847.
39. **Yamasaki, Y., T. Kayashima, H. Soejima, A. Kinoshita, K. Yoshiura, N. Matsumoto, T. Ohta, T. Urano, H. Masuzaki, T. Ishimaru, T. Mukai, N. Niikawa, and T. Kishino.** 2005. Neuron-specific relaxation of *Igf2r* imprinting is associated with neuron-specific histone modifications and lack of its antisense transcript *Air*. Hum. Mol. Genet. **14**:2511–2520.
40. **Yang, Y., T. Li, T. H. Vu, G. A. Ulaner, J. F. Hu, and A. R. Hoffman.** 2003. The histone code regulating expression of the imprinted mouse *Igf2r* gene. Endocrinology **144**:5658–5670.

Human Pathology (2007) 38, 621–628

ELSEVIER

Human PATHOLOGY

www.elsevier.com/locate/humpath

Original contribution

RET oncogene amplification in thyroid cancer: correlations with radiation-associated and high-grade malignancy☆

Masahiro Nakashima MD[a,*], Noboru Takamura MD[e], Hiroyuki Namba MD[b], Vladimir Saenko PhD[c], Serik Meirmanov MD[a], Naomichi Matsumoto MD[d,h], Tomayoshi Hayashi MD[f], Shigeto Maeda MD[g], Ichiro Sekine MD[a]

[a]*Tissue and Histopathology Section, Division of Scientific Data Registry, Atomic Bomb Disease Institute, Nagasaki University Graduate School of Biomedical Sciences, Nagasaki 852-8523, Japan*
[b]*Department of Molecular Medicine, Atomic Bomb Disease Institute, Nagasaki University Graduate School of Biomedical Sciences, Nagasaki 852-8523, Japan*
[c]*Department of International Health and Radiation Research, Atomic Bomb Disease Institute, Nagasaki University Graduate School of Biomedical Sciences, Nagasaki 852-8523, Japan*
[d]*Department of Human Genetics, Atomic Bomb Disease Institute, Nagasaki University Graduate School of Biomedical Sciences, Nagasaki 852-8523, Japan*
[e]*Department of Public Health, Nagasaki University Graduate School of Biomedical Sciences, Nagasaki 852-8523, Japan*
[f]*Department of Pathology, Nagasaki University Hospital, Nagasaki 852-8501, Japan*
[g]*Department of Surgery, Nagasaki University Hospital, Nagasaki 852-8501, Japan*
[h]*Department of Human Genetics, Yokohama City University Graduate School of Medicine, Yokohama 236-0004, Japan*

Received 25 August 2006; revised 12 October 2006; accepted 12 October 2006

Keywords:
Thyroid cancer;
RET amplification;
Radiation;
FISH;
Genomic instability

Summary A radiation etiology is well known in thyroid carcinogenesis. *RET* oncogene rearrangement is the most common oncogenic alteration in Chernobyl-related papillary thyroid cancer (PTC). To find the characteristic alteration associated with *RET* rearrangements in radiation-induced thyroid cancers, we analyzed the *RET* oncogene by fluorescence in situ hybridization. The fluorescence in situ hybridization technique has the possibility of detecting *RET* rearrangements at a single-cell level regardless of the specific fusion partner involved and directly reveals *RET* copy number on a per-cell basis. Our study demonstrated *RET* amplification in all 3 cases of radiation-associated thyroid cancers but not in sporadic well-differentiated PTC (n = 11). Furthermore, *RET* amplification was observed in all 6 cases of sporadic anaplastic thyroid cancers (ATCs). The frequency of *RET* amplification-positive cells was higher in ATC (7.2%-24.1%) than in PTC (1.5%-2.7%). The highest frequency of *RET* amplification-positive cells was observed among ATC cases with a strong p53 immunoreactivity. In conclusion, we found *RET* amplification, which is a rare oncogenic aberration, in thyroid cancer. This report is the first

☆ This work was supported in part through Nagasaki University 21st Century Center of Excellence (COE) program and by Grant for Research Project of Atomic Bomb Diseases from the Japanese Ministry of Health, Labour and Welfare.

* Corresponding author. Tissue and Histopathology Section, Division of Scientific Data Registry, Atomic Bomb Disease Institute, Nagasaki University Graduate School of Biomedical Sciences, Nagasaki 852-8523, Japan.
E-mail address: moemoe@nagasaki-u.ac.jp (M. Nakashima).

0046-8177/$ – see front matter
doi:10.1016/j.humpath.2006.10.013

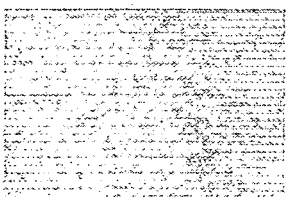

one to suggest the presence of *RET* amplification in PTC and ATC. *RET* amplification was correlated with radiation-associated, high-grade malignant potency, and p53 accumulation, suggesting genomic instability. *RET* amplification might be induced by a high level of genomic instability in connection with progression of thyroid carcinogenesis and, subsequently, be associated with radiation-induced and/or high-grade malignant cases.

1. Introduction

The incidence of papillary thyroid cancer (PTC) was reported to be elevated in both atomic-bomb survivors in Hiroshima and Nagasaki, Japan, and residents living in areas exposed to fallout from the Chernobyl accident, suggesting a radiation etiology in thyroid carcinogenesis. *RET* rearrangement is a well-known molecular alteration observed in PTC. Ret oncoproteins, which function as receptor tyrosine kinases, are dimerized by ligand-binding, activated, and subsequently involved in regulating cell growth and survival in normal tissues [1,2]. During thyroid carcinogenesis, if the 3′ -end of *RET* oncogenes rearrange with other genes containing a coiled-coil domain, they dimerize without ligand stimuli and constitutively activate cell growth and survival in thyroid follicular cells, finally promoting the occurrence of PTC [3-5].

To date, at least 15 different variants of *RET* rearrangement have been reported [6]. *RET* rearrangements are the most common oncogenic alterations in Chernobyl-related PTC; 4 large studies have found that 50% to 90% of Chernobyl-related PTC show *RET* rearrangements—nearly all of them to *RET/PTC1* or *RET/PTC3* [7-10]—resulting from paracentric inversion of chromosome 10 [11]. Although *RET/PTC1* and *RET/PTC3* are most often found in sporadic cases of PTC, their prevalence may vary within a broad range, from 0% to more than 60% [6]. Other less common variants, usually formed as a result of interchromosomal translocation, occur in an extremely limited number of cases. Most often, such translocations have been found in radiation-induced PTC [12]. However, specific molecular alterations have not been identified in radiation-induced PTC.

In the present study, to find the characteristic/specific alterations in *RET* rearrangements in radiation-induced thyroid cancers, we analyzed the *RET* oncogene by fluorescence in situ hybridization (FISH) on paraffin-embedded tissues. Previous studies using FISH analysis of *RET* rearrangements have demonstrated its utility in thyroid cancers [13,14]. The FISH technique can detect *RET* rearrangements at a single-cell level regardless of the specific fusion partner involved and directly reveals *RET* copy number on a per-cell basis.

Here, we describe the presence of *RET* oncogene amplification, which is a rare type of *RET* cytogenetic alteration in PTC. Oncogene amplification is extremely common in human tumors. In thyroid cancers, *RET* oncogene amplification correlated with radiation-induced, high-grade malignancy and anaplastic transformation of PTC. To our knowledge, this is the first report demonstrat-

Table 1 Clinicopathologic profiles of patients and summary of results

Case	Age	Sex	Px	pTNM	Radiation	*RET* rearrangement	*RET* amplification		p53
							Positive cells	Copy no.[a]	
1	32	F	FV	T1N0M0	Tx	Δrfp/ret[b]	1.5%	5.6 (4-8)	-
2	41	F	FV	T4N1bM0	C	PTC3	2.7%	4.8 (3-9)	-
3P	44	M	WD	T1N0M0	-	-	-		-
3R	57	M	ATC	T4N0M0	Tx	-	24.1%	5.2 (3-8)	+
4	64	M	ATC	T3N0M0	-	-	20.3%	6.3 (4-10)	+
5	77	F	ATC	T4N0M0	-	-	19.5%	6.6 (4-8)	+
6	71	F	ATC	T4N1bM0	-	-	13.1%	5.8 (3-8)	-
7	84	F	ATC	T4N0M0	-	-	7.2%	4.8 (3-6)	-
8	78	M	ATC	T4N0M0	-	-	8.9%	5.6 (4-7)	-
9	81	F	ATC	T2N0M0	-	-	10.2%	6.1 (3-7)	-
10	22	F	PD	T4N1aM0	-	PTC1	2.4%	4.5 (4-6)	-
Others (n = 10)	52[c]	F/M (8:2)	WD	T1N0M0	-	-	-		-

Abbreviations: M, male; F, female; Px, pathologic diagnosis; FV, follicular variant PTC; WD, well-differentiated PTC; PD, poorly differentiated PTC; Tx, irradiation therapy; C, Chernobyl case; P, primary; R, recurrent (after irradiation therapy).

[a] Values are shown as mean (range).

[b] Ref [16].

[c] Mean age.

Table 2 List of primers and PCR conditions

Target	Sequence	Annealing (°C)	Amplicon (bp)
RET/PTC1			
Forward	GCCTGGAGGAGCTCACCAA	56	255
Reverse	CTCTGCCTTTCAGATGGAA		
RET/PTC3			
Forward	ACCTGCCAGTGGTTATCAAGCT	58	154
Reverse	TTCGCCTTCTCCTAGAGTTTTTCC		
α-Tubulin			
Forward	AGATCATTGACCTCGTGTTGGA	56	101
Reverse	ACCAGTTCCCCCACCAAAG		

ing *RET* amplification in PTC and anaplastic thyroid cancers (ATC), although *RET* amplification has been reported in medullary thyroid cancer cases [15].

2. Materials and methods

2.1. Subjects

All samples were formalin-fixed paraffin-embedded tissues. The sections were used for FISH analysis and RNA preparation. Three cases of radiation-associated thyroid cancers including 2 cases of PTC and 1 case of anaplastic thyroid cancer (ATC) were explored for *RET* rearrangement by dual-color interphase FISH and reverse transcriptase–polymerase chain reaction (RT-PCR). The clinicopathologic profiles of the 3 radiation-associated cases were as follows: Case 1: a 32-year-old Russian woman received surgical treatment for thyroid cancer that was histologically diagnosed as a follicular variant of PTC. Four years before the surgery, the patient had undergone

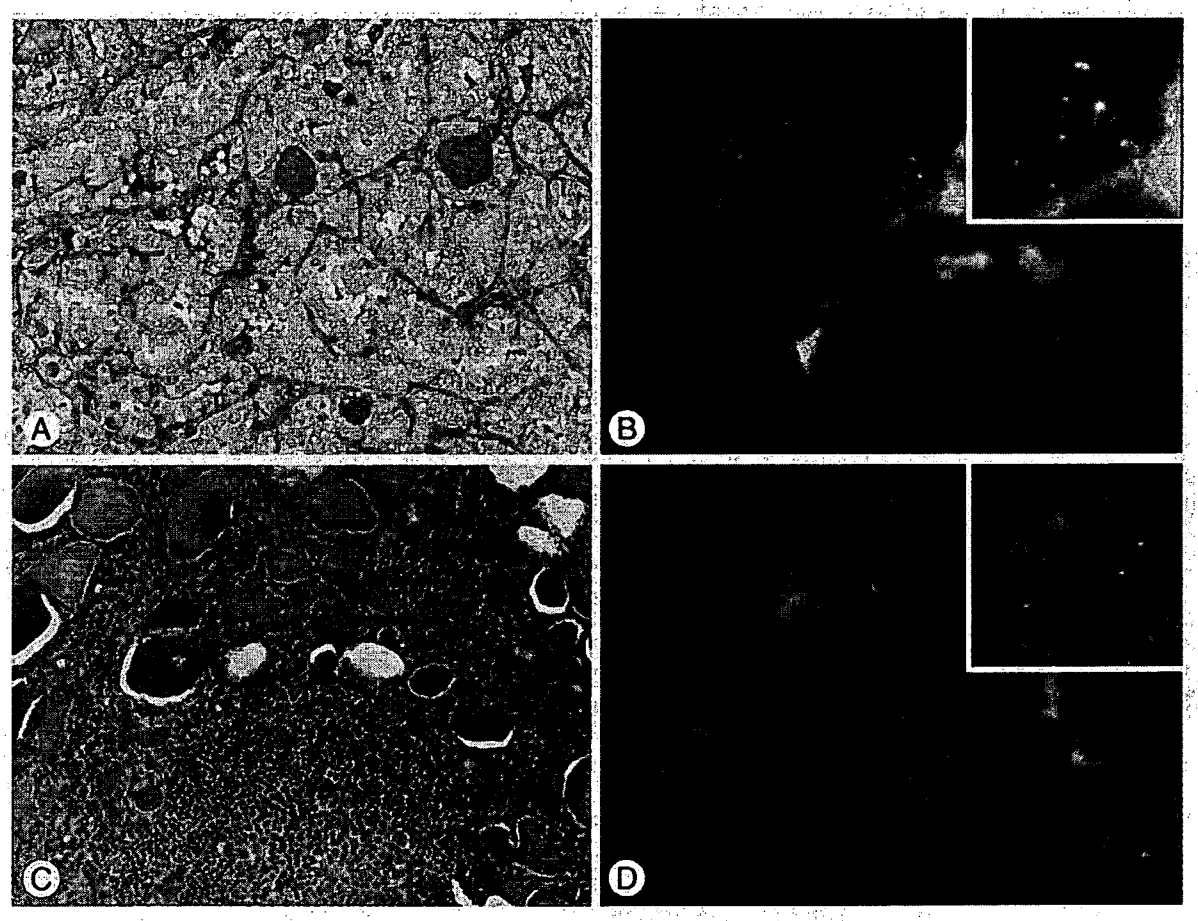

Fig. 1 A case (case 1) of radiation-induced papillary carcinoma, follicular variant (A). FISH analysis demonstrates cancer cells showing 2 *CEP10* and several randomly distributed *RET* signals, suggesting *RET* gene amplification (B). In the nontumor area (C), infiltrating lymphocytes and follicular cells show 2 *RET* signals coupled with 2 *CEP10* signals, suggesting a wild-type *RET* (D).

external radiation therapy (40 Gy) for primary mediastinal lymphoma. A novel tumorigenic rearrangement, *Δrfp/ret*, which was a translocation between chromosomes 6 and 10, was identified as shown in our previous report [16]. Case 2: the patient was a 41-year-old Russian woman living in a radioactively contaminated area around the Chernobyl-accident site; she was 25 years old at the time of the accident and was operated on under the diagnosis of thyroid cancer. A histologic examination revealed it as a follicular variant of PTC. Case 3: a 44-year-old Japanese man was operated on under the diagnosis of thyroid cancer and treated by internal radiation with ^{131}I after the operation. He died of tumor recurrence at 57 years of age. The pathologic diagnosis of the primary cancer was "well differentiated PTC" and that of the recurrent tumor was "ATC." None of these radiation-associated cases received chemotherapy.

As a control in this study, 10 cases of sporadic PTC and 6 cases of sporadic ATC, which had no histories of exposure to atomic bombing, radiation therapy, or chemotherapy, were also analyzed. The clinicopathologic profiles of the patients are summarized in Table 1. The experimental protocol was approved by the Ethics Review Committee of Nagasaki University Graduate School of Biomedical Sciences (Protocol No. 0305150036-2).

2.2. Dual-color interphase FISH

For hybridization, 1 μg DNA of BAC clone RP11-351D16 (accession number AC010864, human chromosome 10q11 containing the *RET* locus) was directly labeled with SpectrumGreen-dUTP by using Nick Translation Kit (Vysis Inc, Downers Grove, Ill) according to the manufacturer's instructions. Deparaffinized sections were heated by microwave in a 0.01 mol/L citrate buffer (pH 6.0) and pretreated with 0.3% pepsin. Subsequently, slides were immersed in 0.1% NP-40 and denatured by heating in 70% formamide/2×SSC. The mixture containing the above-mentioned DNA probes and SpectrumOrange-labeled DNA probes corresponding to the centromere of chromosome 10 (*CEP10*, Vysis Inc) was denatured and applied to the denatured tissue. The slides were covered with a coverslip, sealed with rubber

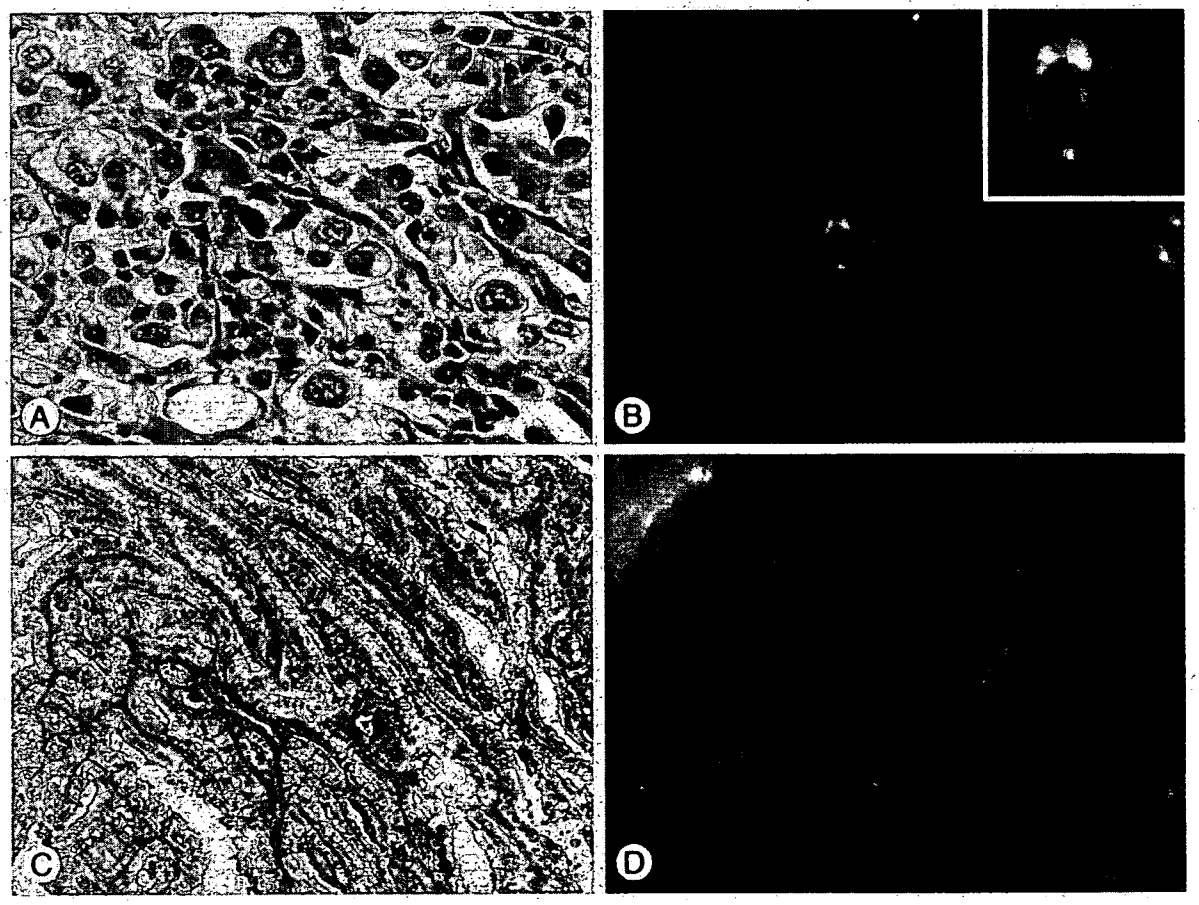

Fig. 2 A case (case 3R) of recurrent anaplastic carcinoma induced by radiation therapy of the primary thyroid tumor (A). FISH analysis demonstrates *RET* amplification in cancer cells (B). The histologic type of the primary tumor (case 3P) was that of a well-differentiated papillary carcinoma (C). A wild type of *RET* signals is evident in this primary cancer (D).

cement, and incubated for 16 hours at 42°C in a humidified chamber. After hybridization, slides were washed, then counterstained and visualized with 4′,6-diamidino-2-phenylindole dihydrochloride (Vysis Inc), and photographed using a fluorescence microscope (Zeiss Axioplan2, Carl Zeiss Japan, Tokyo, Japan) equipped with a CCD camera, and then analyzed with IPLab/MAC image software (Scanalytics Inc, Fairfax, Va). Signals were analyzed in up to 20 viewing areas per case at the 1000-fold magnification.

2.3. Reverse transcriptase–polymerase chain reaction

Total RNA was isolated from tissues with High Pure RNA Paraffin Kit (Roche, Mannheim, Germany) according to the manufacturer's protocol and examined for *RET/PTC1* and *RET/PTC3*. Expressions of *RET/PTC1*, *RET/PTC3*, and *α-tubulin* genes were assessed by RT-PCR using the respective primers designed with the Primer Express Software (PE Applied Biosystems, Foster City, Calif). All reactions were performed with the SuperScript One-Step RT-PCR with Platinum *Taq* System (Invitrogen, Carlsbad, Calif) according to the manufacturer's protocol. Primer sequences, annealing temperature settings in the PCR reactions, and size of amplicons are listed in Table 2.

2.4. Immunohistochemistry

After immersion in 0.3% H_2O_2/methanol, sections were preincubated with 10% normal goat serum. After antigen retrieval, tissues were incubated overnight at 4°C with anti-p53 monoclonal antibody (DO-7, DakoCytomation, Glostrup, Denmark) at a 1:50 dilution. The slides were subsequently incubated with biotinylated goat antimouse IgG antibody for 1 hour, followed by incubation with avidin-peroxidase, and visualized with diaminobenzidine.

3. Results

3.1. Fluorescence in situ hybridization analysis

All results are summarized in Table 1. The FISH analysis for *RET* gene demonstrated nuclei exhibiting several (up to 10) green signals and 2 orange signals in thyroid cancer cells, suggesting amplification of the *RET* gene. All 3 radiation-associated cases—cases 1 (Fig. 1), 2, and 3R (Fig. 2)—showed *RET* amplification, regardless of histologic type and tumor grade; case 1 was a low-grade (pT1N0M0) and case 2 a high-grade (pT4N1bM0) follicular variant of PTC, whereas case 3R was a high-grade (pT4N0M0) ATC. *RET* amplification was also found in all 6 cases of sporadic ATC. On the other hand, in 10 cases of non–radiation-associated PTC, *RET* amplification was evident in only 1 case (case 10; Fig. 3), which was a poorly differentiated and high-grade (pT4N1aM0) PTC from a 22-year-old Japanese woman, whereas the others were of the classical type and low-grade (pT1N0M0) PTC. Although there was no significant difference in the number of extracopies of the gene between cases, the frequency of *RET* amplification-positive cells was higher in ATC (mean, 14.8%; range, 7.2%-24.1%) than in PTC (mean, 2.2%; range, 1.5%-2.7%). The highest frequency of *RET* amplification-positive cells was observed in ATC cases with a strong p53 immunoreactivity (Fig. 4). No *RET* amplification was observed in case 3P (Fig. 2). No *RET* amplification was identified by FISH in normal thyroid follicles surrounding tumors in any of the cases.

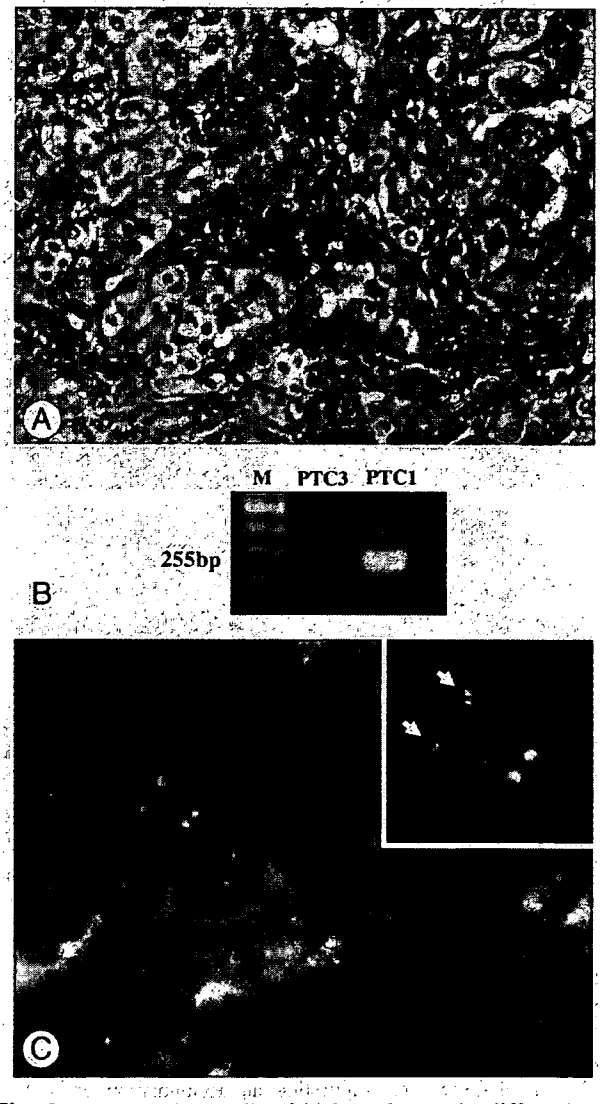

Fig. 3 A case (case 10) of high-grade poorly differentiated carcinoma with no history of radiation exposure (A). RT-PCR reveals *RET/PTC1* rearrangement in this case (B). FISH analysis demonstrates *RET* amplification in cancer cells (C). Two signals in the proximity of the homologous centromere are also observed, suggesting a paracentric inversion of *RET/PTC* rearrangements in the same nuclei (arrows in C).

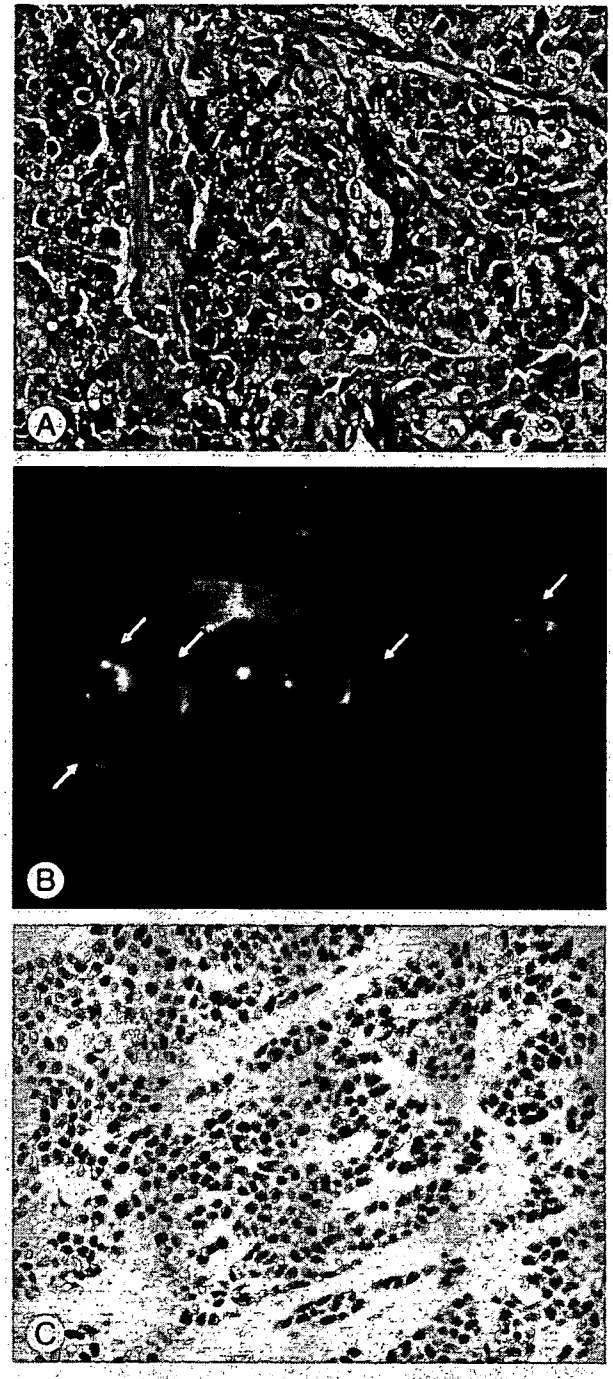

Fig. 4 A case (case 4) of anaplastic carcinoma with no history of radiation exposure (A). In this case, FISH analysis demonstrates several cancer cells showing *RET* amplification (arrows) in a high-power field (B). Immunostaining reveals diffuse and intense p53 immunoreactivity, suggesting an accumulation of mutated p53 proteins (C).

3.2. RT-PCR analysis

RT-PCR analyses revealed *RET/PTC1* and *RET/PTC3* in cases 2 and 10 (Fig. 3C), respectively. Neither *RET/PTC1* nor *RET/PTC3* was demonstrated in other PTC cases or in any ATC cases (data not shown). These results are summarized in Table 1.

3.3. P53 expression

Immunohistochemical results for p53 expression are also shown in Table 1. Intense and diffuse p53 immunoreactivity was evident in the nuclei of cancer cells in 3 cases of ATC, including both a radiation-associated case (case 3R) and 2 sporadic cases (cases 4 and 5), but not in any of the PTC cases. All of the p53-positive ATC cases showed a high frequency (mean, 21.3%; range, 19.5%-24.1%) of *RET* amplification-positive cells (Fig. 4).

4. Discussion

Gene amplification is a term used to indicate the production of multiple copies of a specific gene [17]; it is associated with genomic instability, the main characteristic of cancer cells, and it frequently involves proto-oncogenes [18]. Oncogenes are often amplified in advanced solid tumors, and the amplification correlates with a poor prognosis for patients with ovarian cancer (*HER-2/neu*), breast cancer (*C-MYC, HER-2/neu*), neuroblastoma (*N-MYC*), or small cell lung cancer (*C-MYC*) [19-22]. We found *RET* oncogene amplification in thyroid cancers in vivo. In PTC, *RET* amplification was found in radiation-associated and high-grade cases. Because *RET* amplification was not observed in sporadic, well-differentiated, and low-grade cases of PTC, *RET* amplification could be a molecular marker for radiation-induced and/or high-grade PTC. Furthermore, *RET* amplification was frequently observed in ATC regardless of whether it was a radiation-associated or a sporadic case. In case 3, *RET* amplification was only found in recurrent cancer with anaplastic transformation after irradiation therapy but not in the primary tumor, which was a conventional type PTC. Thus, *RET* amplification may be associated with anaplastic transformation during thyroid tumorigenesis.

Anaplastic thyroid cancer has been reported to arise from preexisting differentiated thyroid cancer [23,24]. In thyroid carcinogenesis, mutations of the *P53* gene are involved in anaplastic and poorly differentiated thyroid carcinomas but not in well-differentiated PTC [25,26]. The cell cycle checkpoint function of wild-type p53 maintains genomic stability and ploidy. Therefore, loss of wild-type p53 functions may be associated with genomic instability—manifested as a complex karyotype during anaplastic transformation—after DNA-damaging chemotherapy and radiation. In our cases, the highest frequency of *RET* amplification-positive cells was observed in ATC cases showing a diffuse p53 overexpression, which included a case of anaplastic transformation after irradiation therapy. These findings suggest that *RET* amplification may be induced by a high level of genomic instability due to *P53* mutation. Interestingly, other authors have also reported

correlations between *P53* aberrations and oncogene amplifications in other solid tumors, such as esophageal, ovarian, bladder, and colorectal cancers [27-30].

Amplification of oncogenes leads to the overexpression of proteins participating in the transduction of growth-related signals and confers a growth advantage to tumor cells during carcinogenesis [31,32]. In such tumors, a majority of cancer cells should express oncogene amplification, suggesting a clonal oncogenesis. However, in our results, *RET* amplification-positive cells were restricted to only a small proportion (1.5%-24.1%) of cells and were never clustering in thyroid cancers. Therefore, we suggest that *RET* amplification is not directly involved in thyroid carcinogenesis, but is rather a randomly induced subclonal event in cancer cells due to a high level of genomic instability associated with progression of cancer stages, which results in intratumoral heterogeneity. A distinct intratumoral heterogeneity has previously been reported for many solid tumors [33-35], suggesting that clonal evolution in such tumors is more complex than predicted by linear models [36]. Similarly, Unger et al [14] have found a heterogeneity in the distribution of *RET* rearrangements in PTC with interphase FISH and have suggested that RET protein does play a role in the generation of tumor, perhaps through paracrine interaction with *RET* rearrangement-negative cells. Furthermore, Zhang et al [37] have demonstrated low-level amplifications of oncogenes, such as *TERT*, *C-MYC*, *CCND1*, and *ERBB2*, which contribute to the development and progression of tumors through different pathways and are frequently detected in cervical cancers. A combination of these amplifications often occurred in different proportions in advanced tumors [37]. Thus, *RET* amplification might play a role in advanced thyroid cancer cooperatively with other oncogenes. Further analyses, such as studies on the expression of the RET protein or mRNA, are required to confirm the oncogenic role of *RET* amplification during thyroid carcinogenesis.

In conclusion, we found *RET* amplification, which is a rare cytogenetic aberration, in thyroid cancer. To the best of our knowledge, this report is the first one to suggest the presence of *RET* oncogene amplification in thyroid cancers other than medullary carcinoma. *RET* amplification was correlated with radiation-associated, high-grade malignant potency and p53 accumulation, suggesting genomic instability. *RET* amplification might be induced by a high level of genomic instability connected with progression of thyroid carcinogenesis and, subsequently, be associated with radiation-induced and/or high-grade malignant cases.

Acknowledgment

The authors are grateful to Prof. Tahara of the Radiation Effects Research Foundation for valuable comments in this study.

Appendix A. Supplementary data

Supplementary data associated with this article can be found, in the online version, at doi:10.1016/j.humpath.2006.10.013.

References

[1] Takahashi M, Buma Y, Iwamoto T, Inaguma Y, Ikeda H, Hiai H. Cloning and expression of the ret proto-oncogene encoding a tyrosine kinase with two potential transmembrane domains. Oncogene 1988; 3:571-8.

[2] Schuchardt A, D'Agati V, Larsson-Blomberg L, Costantini F, Pachnis V. Defects in the kidney and enteric nervous system of mice lacking the tyrosine kinase receptor Ret. Nature 1994;367:380-3.

[3] Grieco M, Santoro M, Berlingieri MT, et al. PTC is a novel rearranged form of the ret proto-oncogene and is frequently detected in vivo in human thyroid papillary carcinomas. Cell 1990;60:557-63.

[4] Jhiang SM, Sagartz JE, Tong Q, et al. Targeted expression of the ret/PTC1 oncogene induces papillary thyroid carcinomas. Endocrinology 1996;137:375-8.

[5] Powell Jr DJ, Russell J, Nibu K, et al. The RET/PTC3 oncogene: metastatic solid-type papillary carcinomas in murine thyroids. Cancer Res 1998;58:5523-8.

[6] Tallini G, Asa SL. RET oncogene activation in papillary thyroid carcinoma. Adv Anat Pathol 2001;8:345-54.

[7] Nikiforov YE, Rowland JM, Bove KE, Monforte-Munoz H, Fagin JA. Distinct pattern of RET oncogene rearrangements in morphological variants of radiation induced and sporadic papillary carcinomas in children. Cancer Res 1997;57:1690-4.

[8] Thomas GA, Bunnell H, Cook HA, et al. High prevalence of RET/PTC rearrangements in Ukrainian and Belarussian post-Chernobyl thyroid papillary carcinomas: a strong correlation between RET/PTC3 and the solid-follicular variant. J Clin Endocrinol Metab 1999; 84:4232-8.

[9] Santoro M, Thomas GA, Vecchio G, et al. Gene rearrangement and Chernobyl related thyroid cancers. Br J Cancer 2000;82:315-22.

[10] Rabes HM, Demidchik EP, Sidorow JD, et al. Pattern of radiation-induced RET and NTRK1 rearrangements in 191 post-Chernobyl papillary carcinomas: biological, phenotypic, and clinical implications. Clin Cancer Res 2000;6:1093-103.

[11] Jhiang SM. The RET proto-oncogene in human cancers. Oncogene 2000;19:5590-7.

[12] Williams D. Cancer after nuclear fallout: lessons from the Chernobyl accident. Nat Rev Cancer 2002;2:543-9.

[13] Corvi R, Martinez-Alfaro M, Harach HR, Zini M, Papotti M, Romeo G. Frequent RET rearrangements in thyroid papillary microcarcinoma detected by interphase fluorescence in situ hybridization. Lab Invest 2001;81:1639-45.

[14] Unger K, Zitzelsberger H, Salvatore G, et al. Heterogeneity in the distribution of RET/PTC rearrangements within individual post-Chernobyl papillary thyroid carcinomas. J Clin Endocrinol Metab 2004;89:4272-9.

[15] Huang SC, Torres-Cruz J, Pack SD, et al. Amplification and overexpression of mutant RET in multiple endocrine neoplasia type 2-associated medullary thyroid carcinoma. J Clin Endocrinol Metab 2003;88:459-63.

[16] Saenko V, Rogounovitch T, Shimizu-Yoshida Y, et al. Novel tumorigenic rearrangement, Δrfp/ret, in a papillary thyroid carcinoma from externally irradiated patient. Mutat Res 2003;527: 81-90.

[17] Brown DD, Dawid IB. Specific gene amplification in oocytes. Oocyte nuclei contain extrachromosomal replicas of the genes for ribosomal RNA. Science 1968;60:272-80.

[18] Zimonjic DB, Zhang H, Shan Z, et al. DNA amplification associated with double minutes originating from chromosome 19 in mouse hepatocellular carcinoma. Cytogenet Cell Genet 2001;93:114-6.
[19] Slamon DJ, Clark GM, Wong SG, Levin WJ, Ullrich A, McGuire WL. Human breast cancer: correlation of relapse and survival with amplification of the HER-2/neu oncogene. Science 1987;235: 177-82.
[20] Slamon DJ, Godolphin W, Jones LA, et al. Studies of the HER-2/neu proto-oncogene in human breast and ovarian cancer. Science 1989; 244:707-12.
[21] Seeger RC, Brodeur GM, Satjer H, et al. Association of multiple copies of the N-myc oncogene with rapid progression of neuroblastomas. N Engl J Med 1985;313:1111-6.
[22] Johnson BE, Battey J, Linnoila I, et al. Changes in the phenotype of human small cell lung cancer cell lines after transfection and expression of the c-myc proto-oncogene. J Clin Invest 1986;78: 525-32.
[23] Nishiyama RH, Dunn EL, Thompson NW. Anaplastic spindle-cell and giant-cell tumors of the thyroid gland. Cancer 1972;30:113-27.
[24] Aldinger KA, Samaan NA, Ibanez M, Hill Jr CS. Anaplastic carcinoma of the thyroid: a review of 84 cases of spindle and giant cell carcinoma of the thyroid. Cancer 1978;41:2267-75.
[25] Ito T, Seyama T, Mizuno T, et al. Unique association of p53 mutations with undifferentiated but not with differentiated carcinomas of the thyroid gland. Cancer Res 1992;52:1369-71.
[26] Donghi R, Longoni A, Pilotti S, Michieli P, Della Porta G, Pierotti MA. Gene p53 mutations are restricted to poorly differentiated and undifferentiated carcinomas of the thyroid gland. J Clin Invest 1993;91:1753-60.
[27] Persons DL, Croughan WS, Borelli KA, Cherian R. Interphase cytogenetics of esophageal adenocarcinoma and precursor lesions. Cancer Genet Cytogenet 1998;106:11-7.
[28] Wang ZR, Liu W, Smith ST, Parrish RS, Young SR. c-Myc and chromosome 8 centromere studies of ovarian cancer by interphase FISH. Exp Mol Pathol 1999;66:140-8.
[29] Mahdy E, Pan Y, Wang N, Malmstrom PU, Ekman P, Bergerheim U. Chromosome 8 numerical aberration and C-MYC copy number gain in bladder cancer are linked to stage and grade. Anticancer Res 2001;21:3167-73.
[30] Ozakyol A, Ozdemir M, Artan S. Fish detected p53 deletion and N-MYC amplification in colorectal cancer. Hepatogastroenterology 2006;53:192-5.
[31] Stark GR, Debatisse M, Giulotto E, Wahl GM. Recent progress in understanding mechanisms of mammalian DNA amplification. Cell 1989;57:901-8.
[32] Snapka RM. Gene amplification as a target for cancer chemotherapy. Oncol Res 1992;4:145-50.
[33] Walch AK, Zitzelsberger HF, Bruch J, et al. Chromosomal imbalances in Barrett's adenocarcinoma and the metaplasia-dysplasia-carcinoma sequence. Am J Pathol 2000;156:555-66.
[34] Aubele M, Malttis A, Zitzelsberger H, et al. Intratumoral heterogeneity in breast carcinoma revealed by laser-microdissection and comparative genomic hybridization. Cancer Genet Cytogenet 1999;110:94-102.
[35] Zitzelberger H, Kulka U, Lehmann L, et al. Genetic heterogeneity in a prostatic carcinoma and associated prostatic intraepithelial neoplasia as demonstrated by combined use of laser-microdissection, degenerate oligonucleotide primed PCR and comparative genomic hybridization. Virchows Arch 1998;433:297-304.
[36] Barrett MT, Sanchez CA, Prevo LJ, et al. Evolution of neoplastic cell lineages in Barrett esophagus. Nat Genet 1999;22:106-9.
[37] Zhang A, Månér S, Betz R, et al. Genetic alterations in cervical carcinomas: frequent low-level amplifications of oncogenes are associated with human papilloma virus infection. Int J Cancer 2002; 101:427-33.

American Journal of Medical Genetics Part A 143A:546–552 (2007)

Congenital Arhinia:
Molecular-Genetic Analysis of Five Patients

Daisuke Sato,[1,2,3] Osamu Shimokawa,[1,3,4] Naoki Harada,[3,4] Oystein E. Olsen,[5] Jia-Woei Hou,[6] Wolfgang Muhlbauer,[7] Ellen Blinkenberg,[8] Nobuhiko Okamoto,[9] Akira Kinoshita,[1] Naomichi Matsumoto,[3,10] Shinji Kondo,[3,11] Tatsuya Kishino,[3,11] Nobutomo Miwa,[1,3] Tadashi Ariga,[2] Norio Niikawa,[1,3] and Koh-ichiro Yoshiura[1,3]*

[1]Department of Human Genetics, Nagasaki University Graduate School of Biomedical Sciences, Nagasaki, Japan
[2]Department of Pediatrics, Hokkaido University Graduate School of Medicine, Sapporo, Japan
[3]Solution Oriented Research of Science and Technology (SORST), Japan Science and Technology Agency (JST), Kawaguchi, Japan
[4]Kyushu Medical Science, Nagasaki, Japan
[5]Department of Radiology, Great Ormond Street Hospital for Children, London, UK
[6]Division of Medical Genetics, Department of Pediatrics, Chang Gung Children's Hospital, Taoyuan, Taiwan
[7]Plastic Surgery Arabella, Munich, Germany
[8]Center for Medical Genetics and Molecular Medicine, Haukeland University Hospital, Bergen, Norway
[9]Department of Planning and Research, Osaka Medical Center and Research Institute for Maternal and Child Health, Izumi, Japan
[10]Department of Human Genetics, Yokohama City Graduate School of Medicine, Yokohama, Japan
[11]Division of Functional Genomics, Center for Frontier Life Sciences, Nagasaki University, Nagasaki, Japan

Received 30 May 2006; Accepted 30 October 2006

Congenital arhinia, complete absence of the nose, is an extremely rare anomaly with unknown cause. To our knowledge, a total of 36 cases have been reported, but there has been no molecular-genetic study on this anomaly. We encountered a sporadic case of congenital arhinia associated with a de novo chromosomal translocation, t(3;12)(q13.2;p11.2). This led us to analyze the patient by BAC-based FISH for translocation breakpoints and whole-genome array CGH for other possible deletions/duplications in the genome. We found in this patient an approximately 19 Mb deletion spanning from 3q11.2 to 3q13.31 but no disruption of any gene(s) at the other breakpoint, 12p11.2. As the deleted segment at 3q was a strong candidate region containing the putative arhinia gene, we also performed the array CGH in four other arhinia patients with normal karyotypes, as well as mutation analysis of two genes, *COL8A1* and *CPOX*, selected among hundreds of genes located to the deleted region, because they are expressed during early stages of human craniofacial development. However, in the four patients, there were no copy number aberrations in the region examined or no mutations in the two genes. Although our study failed to identify the putative arhinia gene, the data may become a clue to unravel the underlying mechanism of arhinia. © 2007 Wiley-Liss, Inc.

Key words: arhinia; translocation breakpoint; deletion; 3q; 12p; FISH; array CGH

How to cite this article: Sato D, Shimokawa O, Harada N, Olsen OE, Hou J-W, Muhlbauer W, Blinkenberg E, Okamoto N, Kinoshita A, Matsumoto N, Kondo S, Kishino T, Miwa N, Ariga T, Niikawa N, Yoshiura K-i. 2007. Congenital arhinia: Molecular-genetic analysis of five patients. Am J Med Genet Part A 143A:546–552.

INTRODUCTION

Congenital arhinia, complete absence of the nose, is an extremely rare abnormality with unknown cause. Congenital arhinia is often associated with microphthalmia, choanal atresia, and/or cleft palate [Graham and Lee, 2006]. To the best of our knowledge, only 36 cases of arhinia have been reported [Ruprecht and Majewski, 1978; Kaminker et al., 1985; Cohen and Goitein, 1986; Sakai et al., 1989; Galetti et al., 1994; Onizuka et al., 1995; Thiele et al., 1996;

Grant sponsor: Grants-in-Aid for Scientific Research; Grant number: 13854024; Grant sponsor: Applied Genomics; Grant numbers: 17019055, 17590288; Grant sponsor: Ministry of Education, Culture, Sports, Science and Technology (MEXT) of Japan; Grant sponsor: SORST (Japan Science and Technology Agency, JST).

*Correspondence to: Koh-ichiro Yoshiura, MD, PhD, Department of Human Genetics, Nagasaki University Graduate School of Biomedical Sciences, Sakamoto 1-12-4, Nagasaki 852-8523, Japan.
E-mail: kyoshi@net.nagasaki-u.ac.jp

DOI 10.1002/ajmg.a.31613

Choi et al., 1998; Cusick et al., 2000; Olsen et al., 2001; McGlone, 2003; Hou, 2004; Jules et al., 2004; Mathur et al., 2005; Shino et al., 2005; Graham and Lee, 2006]. Most cases were sporadic, but two familial cases were also reported [Ruprecht and Majewski, 1978; Thiele et al., 1996]. As two sisters with arhinia and microphthalmia were born to non-consanguineous parents, an autosomal recessive mode of inheritance has been suggested in this family [Ruprecht and Majewski, 1978]. In the other family, an aunt and a niece were affected with arhinia, suggesting a dominant mode of inheritance with reduced penetrance [Thiele et al., 1996]. Of the 17 patients who were karyotyped, 14 had a normal karyotype, whereas three cases had 46,XX/47,XX,+9 [Kaminker et al., 1985], inv(9) [Cohen and Goitein, 1986], or t(3;12)(q13.2;p11.2) [Hou, 2004]. These findings may indicate that genetic factors play a role in the occurrence of arhinia. Several genes have been proposed as candidates for arhinia, such as *PAX6* and its downstream targets, those of the FGF signaling, *MSX1*, *NRP2*, *GSC*, *ALX3*, and *ALX4* [Hou, 2004; Graham and Lee, 2006]. However, no genetic analysis has yet been undertaken. A de novo balanced reciprocal chromosomal translocation with a congenital disorder provides a good opportunity to discover the gene causing the disease [Mizuguchi et al., 2004].

We previously encountered a patient with congenital arhinia, small eyes and other abnormalities who was cytogenetically diagnosed to have a translocation, t(3;12)(q13.2;p11.2) [Hou, 2004]. Under a hypothesis that a gene responsible for arhinia is disrupted at either of the breakpoints of the translocation, we performed breakpoint analysis of the patient as well as genome analyses of four other patients with arhinia.

MATERIALS AND METHODS

Subjects

This study was approved by the Committee for Ethical Issues on Human Genome and Gene Analysis, Nagasaki University. Five patients with arhinia were collected and analyzed as a collaboration study among six medical institutions (Nagasaki University Graduate School of Biomedical Sciences, Nagasaki, Japan; Great Ormond Street Hospital for Children, London, UK; Chang Gung Children's Hospital, Taoyuan, Taiwan; Plastic Surgery Arabella, Munich, Germany; Center for Medical Genetics and Molecular Medicine, Haukeland University Hospital, Bergen, Norway; and Osaka Medical Center and Research Institute for Maternal and Child Health, Osaka, Japan). Clinical findings of these five patients are shown in Table I. One patient (Patient A) had a de novo translocation, t(3;12)(q13.2;p11.2) and the other four patients (Patients B–E) were karyotypically normal.

We first focused our interest on Patient A and carried out a breakpoint analysis to try to isolate the

TABLE I. Clinical Findings of Five Patients With Arhinia

	Patients [References]				
	A	B	C	D	E
Clinical findings	[Hou, 2004]	[Okamoto, unpublished]	[Muhlbauer et al., 1993]	[Olsen et al., 2001]	[Sakai et al., 1989]
Sex	F	M	F	F	M
Karyotype	46,XX,t(3;12)(q13.2;p11.2)	46,XY	46,XX	46,XX	46,XY
High arched palate	+	+	+	+	+
Hypertelorism	+	+	+	+	+ (pseudo)
Microphthalmia	Bilateral	Left	NA	NA	–
Coloboma iris	+	Left	NA	Bilateral	–
Published					
Development	NA	N	N	N	N
Brain imaging	N	N	N	N	N
Olfactory bulbs	–	–	NA	–	NA
Family history	–	–	–	–	–
Pregnancy	UN	UN	UN	PH	NA
Birth weight (g)	2,800	2,368	2,640	3,070	3,346
Paranasal sinuses	UD	+	–	–	NA
Nasolacrimal ducts	NA	–	–	–	–
Complications	Scoliosis, epilepsy	Hypogonadism, autism	–	–	–
Current status	Living DD GR	Living	Living ND GR NNB	Unknown	Living

F, female; M, male; +, observed; –, not observed; NA, not assessed; N, normal; UN, uneventful; PH, polyhydramnios; UD, underdeveloped; DD, delayed development; ND, normal development; GR, growth retardation; NNB, no nasal breathing.

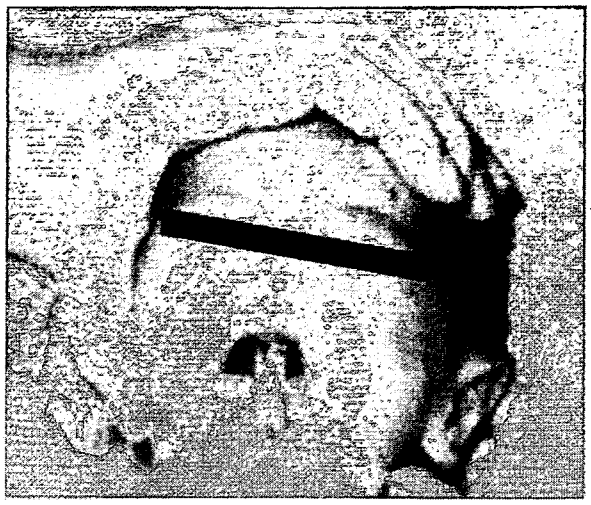

FIG. 1. Patient B at age 6 days, showing the absence of the nose.

putative arhinia gene. Detailed clinical features of Patients A, C, D, and E were reported previously [Sakai et al., 1989; Muhlbauer et al., 1993; Olsen et al., 2001; Hou, 2004, respectively]. Patient B was a Japanese boy whose clinical manifestations have been unpublished. He was born to healthy and non-consanguineous parents by cesarean at 39 weeks of gestation with a birth weight of 2,368 g, length 48 cm, and OFC of 33.7 cm (Fig. 1). Because of his congenital arhinia, a nasal airway was created by a surgical operation at age 17 days to facilitate oral feeding. Other clinical manifestations included bilateral microphthalmia, coloboma of the iris, mid-face hypoplasia, high arched palate, hypertelorism, and absent nasolacrimal ducts. He had neither cleft palate nor low set ears. At age 4 years, his weight was 12.7 kg, height 94.7 cm, and OFC 50 cm, and had paranasal sinuses, normal hearing acuity, autistic behavior, and hypogonadotropic hypogonadism. He is currently able to eat foods through his mouth by himself. His psychomotor developmental quotient was estimated at 65.

Fluorescence In Situ Hybridization (FISH) Analysis

Metaphase chromosomes were prepared from an immortalized lymphoblastoid cell line according to the standard protocol [Shimokawa et al., 2005]. The RPCI-11 human BAC clones mapped around the breakpoints, 3q13.2 and 12p11.2, were selected and used for FISH analyses. Mapping information was retrieved from the UCSC genome browser, 2003 July version (http://genome.ucsc.edu/cgi-bin/hgGateway). BAC-clone DNA was extracted using an automatic DNA extraction system (Kurabo, Osaka, Japan) and labeled with SpectrumGreen-11-dUTP or SpectrumOrange-11-dUTP (Vysis, Downers Grove, IL) by nick translation. Fluorescent probes were hybridized to metaphase chromosomes for 16–72 hr, and then chromosome slides were washed and counterstained with DAPI using standard protocols [Shimokawa et al., 2005]. Fluorescence signals were observed under Zeiss Axioskop microscope equipped with a quad filter set with single-band excitation filters (84000, Chroma Technology Corporation, Brattleboro, VT). Images were captured by cooled CCD camera (TEA/CCD-1317-G1, Princeton Instruments, Trenton, NJ) and merged with IPLab/MA.

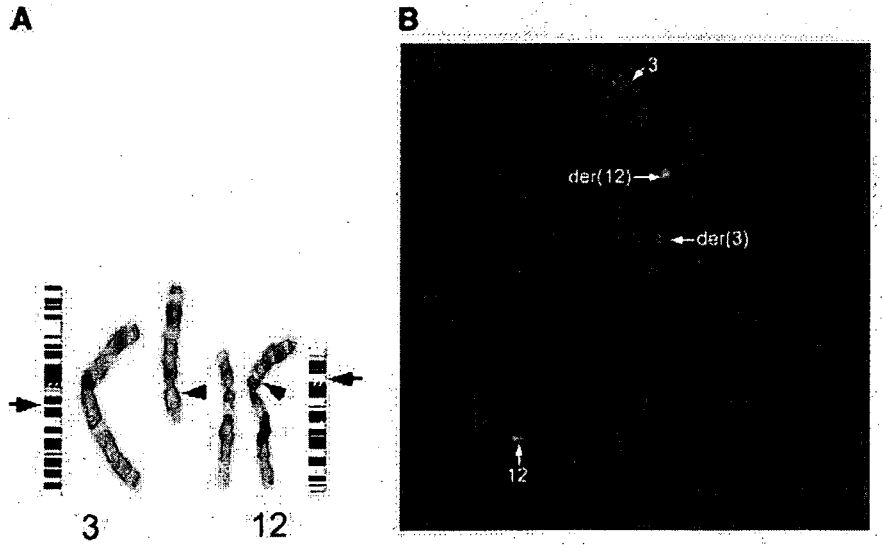

FIG. 2. A: Partial karyotype of Patient A. Arrows and arrowheads show the breakpoints. B: FISH analysis in Patient A. Green signals for a BAC clone, RP11-55L17, that spans the 12p breakpoint appear on der(3), der(12) and normal chromosome 12, while red signals for a chromosome 3-derived clone, RP11-803P6, are seen only on normal chromosome 3. The findings indicate a deletion only in der(3).

Array Comparative Genomic Hybridization (CGH)

DNA was extracted from peripheral blood lymphocytes by conventional method [Sambrook and Russell, 2001]. To detect chromosomal aberrations, we performed homemade whole-genome BAC-based array CGH (array CGH) using genomic DNA of all five patients according to the method described previously [Miyake et al., 2006]. The microarray contains 2,173 BAC and PAC clones which span the whole genome at each of 1.5 Mb average.

Mutation Analysis

A screening for mutations of *COL8A1* and *CPOX* was performed in the four arhinia patients with normal karyotypes. All exon sequences and their flanking intron sequences of the two genes were amplified by PCR for direct sequencing. PCR conditions were set at 40 cycles of 94°C for 30 sec, 62°C for 30 sec, and 72°C for 45 sec in a 15 μl mixture containing 1× PCR buffer with 1.5 mM $MgCl_2$, 0.2 mM each of dNTP, 1 μM each primer and 0.4 Units Taq polymerase (TaKaRa, Otsu, Japan). PCR products were treated with ExoSAP-IT (Amersham Biosciences, Piscateway, NJ) and both strands were sequenced with BigDye Terminator Sequencing kit version 3.1 according to the supplied protocol (Applied Biosystems, Foster City, CA). The reaction mixture was purified using Sephadex G-50 superfine (Amersham Biosciences) and analyzed on the ABI Genetic Analyzer 3100 (Applied Biosystems) with the Sequence Analysis software (Applied Biosystems) and aligned with the Auto Assembler version2.1.1 software (Applied Biosystems) to find DNA alterations.

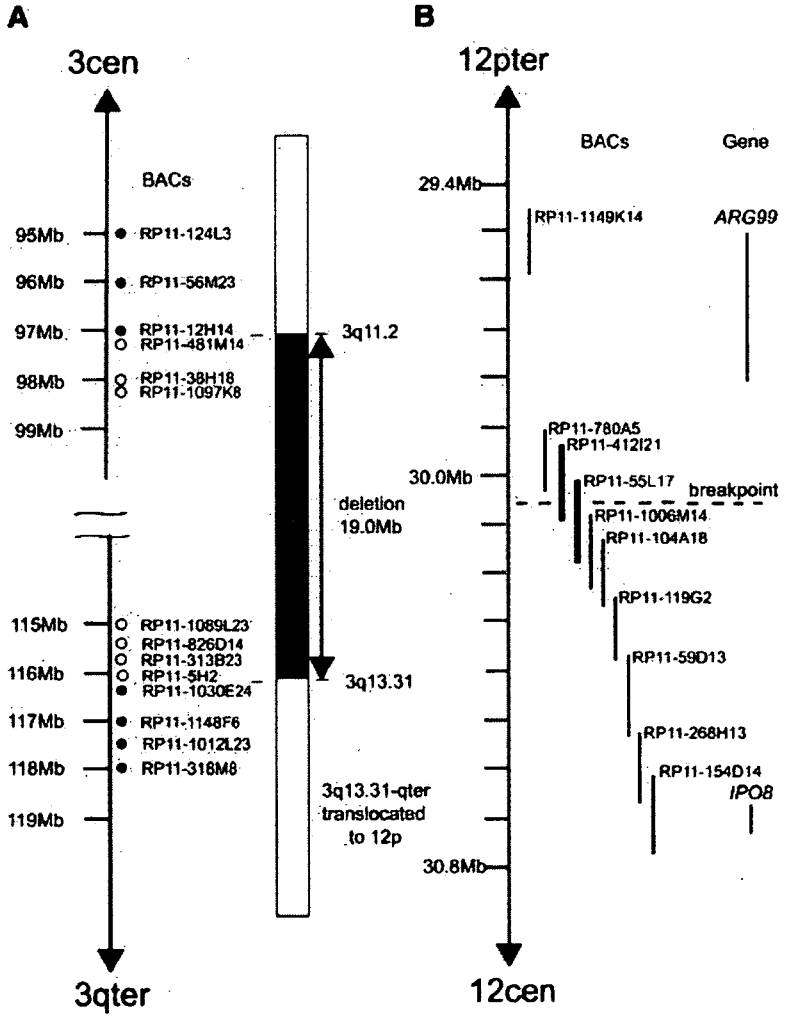

FIG. 3. A: Physical map covering the 3q11.2–3q13.31 deleted region of Patient A. Solid and open circles indicate the presence and absence of clones in Patient A, respectively. B: Physical map of the 12p11 breakpoint region. Thick lines indicate BAC clones covering the breakpoint. Genes *ARG99* and *IPO8* are located close to the breakpoint.

RESULTS AND DISCUSSION

Although the translocation of Patient A looked balanced (Fig. 2A) [Hou, 2004], there was actually a relatively large deletion at the 3q13.2 breakpoint region of her derivative chromosome 3. FISH analysis revealed that the 3q proximal end of the deleted segment was confined to 3q11.2 between BAC clones, RP11-12H14, and RP11-481M14, and the distal end to 3q13.31 between RP11-5H2 and RP11-1030E24 (Figs. 2B and 3). Since lacking signals were confirmed for 16 other BACs that are located between the two ends, the deletion extended to approximately 19 Mb in size from 3q11.2 to 3q13.31 (UCSC Genome Browser). As for the other derivative chromosome 12, as two neighbor BAC clones, RP11-412I21, and RP11-55L17, in a contig were identified to cover the 12p11.22 breakpoint, there was no deletion at the breakpoint.

To know whether any other chromosomal aberrations exist in the genome of the five patients examined, whole-genome array CGH was performed. Consequently, the array CGH confirmed in Patient A the presence of the 3q deletion (Fig. 4) without deletions or duplications in any other chromosomes. In Patient D, four regions were suspected to have duplication, but this could not be confirmed by subsequent FISH, because her chromosome preparation was not available. There was no chromosomal aberration in the remaining three patients.

A literature search for deletions for 3q11.2–3q13.31 found eight reported cases [Arai et al., 1982; Jenkins et al., 1985; McMorrow et al., 1986; Okada et al., 1987; Fujita et al., 1992; Genuardi et al., 1994; Ogilvie et al., 1998]. The smallest region of overlap (SRO) for deletion among them is almost confined to 3q12–3q13.31 (Fig. 5). The deletion in one patient (Case 8 in Fig. 5) [Jenkins et al., 1985] was reported to lie between 3q11 and 3q21. However, the exact location of the proximal border in this patient was not clear since either FISH or molecular analysis was not carried out. None but one patient [Arai et al., 1982] had any nose anomaly, and none of the eight patients manifested microphathalmia that is virtually accompanied with arhinia [Graham and Lee, 2006]. The exceptional patient whose deletion involved 3q13–q21 (Case 7, Fig. 5) had alobar holoprosencephaly, arhinia, and cleft lip [Arai et al., 1982]. Although arhinia of this case seems atypical and to be a holoprosencephaly-associated median facial anomaly, the patient might provide possible information for localization of the arhinia locus. If the locus exists at the long arm of chromosome 3, it might be confined to a segment between 3q11.2 and the proximal border of the deletion of Case 8

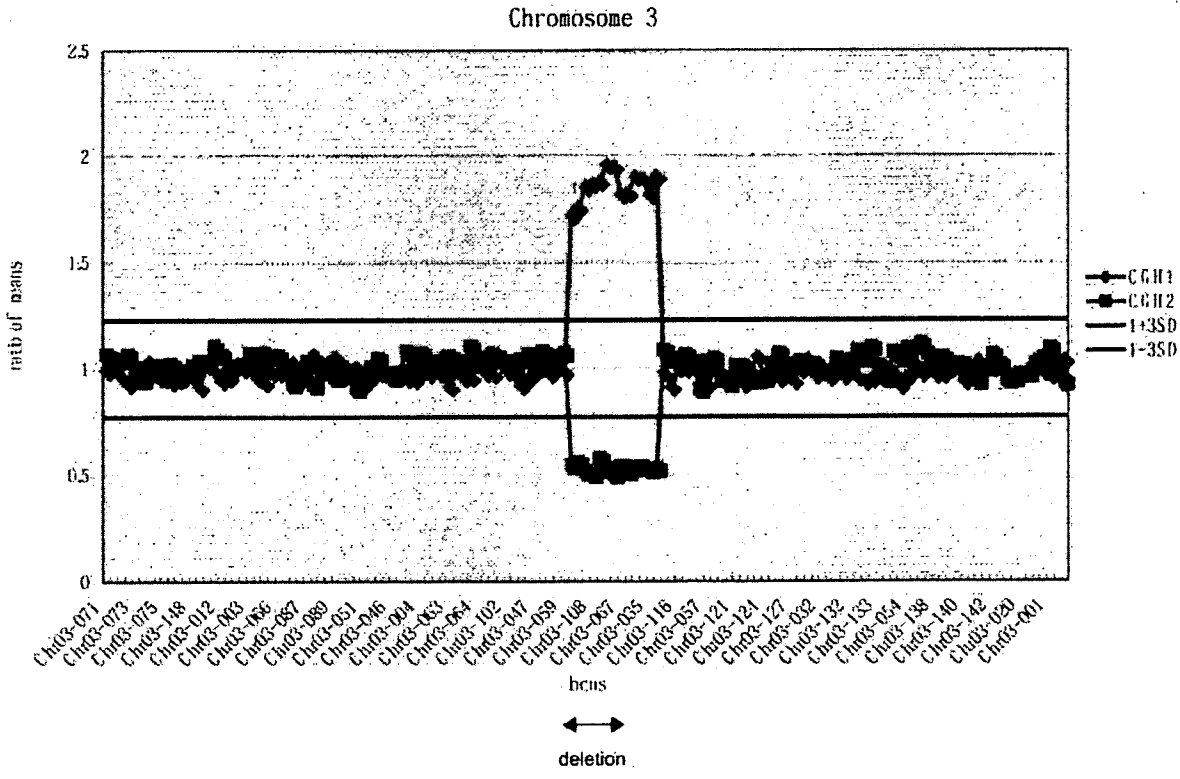

FIG. 4. Array CGH analysis in Patient A, showing a deletion on 3q. The clone at the proximal end within the deletion was RP11-262O19 (3q11.2), and the distal end clone was RP11-342J15 (3q13.31), the results suggesting that the deletion is approximately 18 Mb in size.

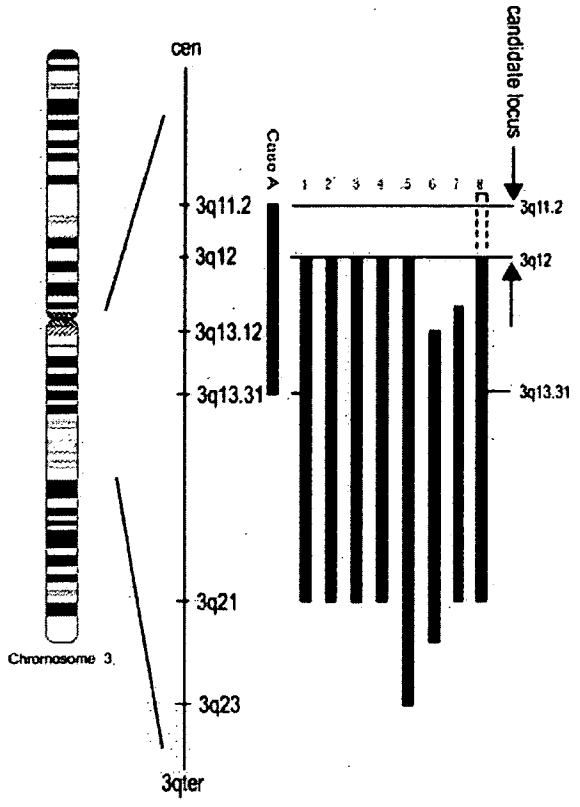

FIG. 5. Extent (bars) of 3q11.2–3q13.31 deletion in Patient A and eight reported cases. **Lanes 1–8** are from McMorrow et al. [1986], Ogilvie et al. [1998], Okada et al. [1987], Fujita et al. [1992], Genuardi et al. [1994], Arai et al. [1982], and Jenkins et al. [1985], respectively.

(Fig. 5). We selected two genes, *COL8A1* and *CPOX*, from 3q11.2 within the deletion of Patient A, and analyzed for their mutations in Patients B–E. According to the Craniofacial and Oral Gene Expression Network (COGENE, http://hg.wustl.edu/COGENE/index.html), *COL8A1* and *CPOX* are expressed in the frontnasal prominence at the 4th week, and between the 4th and 5th weeks, respectively, suggesting they play some roles in the nasal development. However, there was no pathogenomonic mutation of *COL8A1* or *CPOX* in the four arhinia patients with normal karyotypes.

As for the other breakpoint of Patient A, we have confirmed that any known genes were not disrupted at 12p11.22. Two genes, *ARG99* and *IPO8*, located near the breakpoint, seem to have no functions related to the human nasal development. However, it cannot totally be ruled out that there may be unknown RNA transcript(s) on the breakpoint or the breakage may affect a long-distance position effect [Velagaleti et al., 2005].

The nasal placode, the anlage of the nose, begins to develop from the 12th to the 13th Carnegie stage, at the end of the fourth embryonic week. The stage between the end of the 4th week to the 7th week is the most active, important period in the human nose development [O'Rahilly, 1967; Kim et al., 2004]. A failure of the developmental process may result in arhinia, for example, failure of growth or overgrowth of the medial and lateral nasal process sequentially leads to premature fusion of the medial nasal processes [Albernaz et al., 1996].

In conclusion, analysis of five patients with arhinia revealed, although a 19 Mb large deletion involving 3q11–q13 was identified in one patient, no chromosome aberrations or gene mutations were found in the other four patients. Nevertheless, our findings may become a clue to isolate the putative arhinia gene. Further molecular studies in new patients, as well as that on other genes within the deleted region in Patient A, are needed to unravel the underlying cause of arhinia. This is the first report of molecular-genetic study on congenital arhinia.

ACKNOWLEDGMENTS

Participation of all patients in this study is highly appreciated. We also thank Ms Y. Noguchi, K. Miyazaki and A. Goto for their technical assistance. This study was supported by Grants-in-Aid for Scientific Research (Category S, No. 13854024 and Priority Areas—Applied Genomics, No. 17019055 for N. N.; and No. 17590288 for K. Y.) from the Ministry of Education, Culture, Sports, Science and Technology (MEXT) of Japan, and by SORST from the Japan Science and Technology Agency (JST) for N. N.

REFERENCES

Albernaz VS, Castillo M, Mukherji K, Ihmeidan IH. 1996. Congenital arhinia. Am J Neuroradiol 17:1312–1314.

Arai K, Matukiyo H, Takazawa H. 1982. A case report of partial deletion of the long arm of the No.3 chromosome. Med Genet Res 4:1–4.

Choi S, Shiozu H, Sato K, Nishida H. 1998. A case report of congenital arhinia. Acta Neonatol Jpn 34:83–86.

Cohen D, Goitein K. 1986. Arhinia. Rhinology 24:287–292.

Cusick W, Sullivan CA, Rojas B, Poole AE, Poole DA. 2000. Prenatal diagnosis of total arhinia. Ultrasound Obstet Gynecol 15:259–261.

Fujita H, Meng J, Kawamura M, Tozuka N, Ishii F, Tanaka N. 1992. Boy with a chromosome del(3)(q12q23) and blepharophimosis syndrome. Am J Med Genet 44:434–436.

Galetti R, Dallari S, Bruzzi M, Vincenzi A, Galetti G. 1994. Consideration on respiratory physiopathology in a case of total arhinia. Acta Otorhinol Ital 14:63–69.

Genuardi M, Calvieri F, Tozzi C, Coslovi R, Neri G. 1994. A new case of interstitial deletion of chromosome 3q,del(3q)(q13.12q21.3), with agenesis of the corpus callosum. Clin Dysmorphol 3:292–296.

Graham JM, Lee J. 2006. Bosma arhinia microphthalmia syndrome. Am J Med Genet Part A 140A:189–193.

Hou JW. 2004. Congenital arhinia with de novo reciprocal translocation, t(3;12)(q13.2;p11.2). Am J Med Genet Part A 130A:200–203.

Jenkins MB, Stang HJ, Davis E, Boyd L. 1985. Deletion of the proximal long arm of chromosome 3 in an infant with features of Turner syndrome. Ann Génét (Paris) 28:42–44.

Jules AF, Cynthia MG, Terry T, Samue S, Brian S, Larry H. 2004. Vertical facial distraction in the treatment of arhinia. Plast Reconstr Surg 113:2061–2066.

Kaminker CP, Dain L, Lamas MA, Sanchez JM. 1985. Mosaic trisomy 9 syndrome with unusual phenotype. Am J Med Genet 22:237–241.

Kim CH, Park HW, Kim K, Yoon JH. 2004. Early development of the nose in human embryos: A stereomicroscopic and histologic analysis. Laryngoscope 114:1791–1800.

Mathur NN, Dubey NK, Kumar S, Bothra R, Chadha A. 2005. Arhinia. Int J Pediatr Otorhinolaryngol 69:97–99.

McGlone L. 2003. Congenital arhinia. J Paediatr Child health 39:474–476.

McMorrow LE, Reid CS, Coleman J, Medeiros A, D'Andrea M, Santucci T, McCormack MK. 1986. A new interstitial deletion of the long arm of chromosome 3. Am J Hum Genet 39: A124.

Miyake N, Shimokawa O, Harada N, Sosonkina N, Okubo A, Kawara H, Okamoto N, Ohashi H, Kurosawa K, Naritomi K, Kaname T, Nagai T, Shotelersuk V, Hou JW, Fukushima Y, Kondoh T, Matsumoto T, Shinoki T, Kato M, Tonoki H, Nomura M, Yoshiura K, Kishino T, Ohta T, Niikawa N, Matsumoto N. 2006. No detectable genomic aberrations by BAC array CGH in Kabuki make-up syndrome patients. Am J Med Genet Part A 140A:291–293.

Mizuguchi T, Collod-Beroud G, Akiyama T, Harada N, Morisaki T, Abifadel M, Allard D, Varret M, Claustres M, Ihara M, Kinoshita A, Yoshiura K, Junien C, Kajii T, Jondeau G, Niikawa N, Boileau C, Matsumoto N. 2004. Heterozygous *TGFBR2* mutations in Marfan syndrome. Nat Genet 36:855–860.

Muhlbauer W, Schmidt A, Fairley J. 1993. Simultaneous construction of an internal and external nose in an infant with arhinia. Plast Reconstr Surg 91:720–725.

O'Rahilly R. 1967. The early development of the nasal pit in staged human embryos. Anat Rec 157:380.

Ogilvie CM, Rooney SC, Hodgson SV, Berry AC. 1998. Deletion of chromosome 3q proximal region gives rise to a variable phenotype. Clin Genet 53:220–222.

Okada N, Hasegawa T, Osawa M, Fukuyama Y. 1987. A case of de novo interstitial deletion 3q. J Med Genet 24:305–308.

Olsen OE, Gjelland K, Reigstad H, Rosendahl K. 2001. Congenital absence of the nose: A case report and literature review. Pediatr Radiol 31:225–232.

Onizuka T, Ohkubo F, Hosaka Y, Ichinose M, Keiko Okazaki K. 1995. Arhinia: A case report. Worldplast 1:65–71.

Ruprecht KW, Majewski F. 1978. Familial arhinia combined with Peter's anomaly and maxillar deformities, a new malformation syndrome? Klin Mbl Augenheilk 172:708–715.

Sakai Y, Ohara Y, Inoue Y. 1989. Congenital complete absence of the nose. J Jpn Plast Reconstr Surg 9:265–273.

Sambrook J, Russell DW. 2001. Molecular cloning: A laboratory manual. Cold Spring Harbor, New York: Cold Spring Harbor Laboratory Press.

Shimokawa O, Miyake N, Yoshimura T, Sosonkina N, Harada N, Mizuguchi T, Kondoh S, Kishino T, Ohta T, Remco V, Takashima T, Kinoshita A, Yoshiura K, Niikawa N, Matsumoto N. 2005. Molecular characterization of del(8)(p23.1p23.1) in a case of congenital diaphragmatic hernia. Am J Med Genet Part A 136A:49–51.

Shino M, Chikamatsu K, Yasuoka Y, Nagai K, Furuya N. 2005. Congenital arhinia: A case report and functional evaluation. Laryngoscope 115:1118–1123.

Thiele H, Musil A, Nagel F, Majewski F. 1996. Familial arhinia, choanal atresia, and microphthalmia. Am J Med Genet 63:310–313.

Velagaleti GVN, Bien-Willner GA, Northup JK, Lockhart LH, Hawkins JC, Jalal SM, Withers M, Lupski JR, Stankiewicz P. 2005. Position Effects due to chromosome breakpoints that map ~900 kb upstream and ~1.3 Mb downstream od SOX9 in two patients with Campomelic dysplasia. Am J Hum Genet 76:652–662.

American Journal of Medical Genetics Part A 143A:694–698 (2007)

FBN2, *FBN1*, *TGFBR1*, and *TGFBR2* Analyses in Congenital Contractural Arachnodactyly

Akira Nishimura,[1] Haruya Sakai,[1] Shiro Ikegawa,[2] Hiroshi Kitoh,[3] Nobuyuki Haga,[4] Satoshi Ishikiriyama,[5] Toshiro Nagai,[6] Fumio Takada,[7] Takako Ohata,[1,7] Fumihiko Tanaka,[8] Hotaka Kamasaki,[9] Hirotomo Saitsu,[1] Takeshi Mizuguchi,[1] and Naomichi Matsumoto[1]*

[1]Department of Human Genetics, Yokohama City University Graduate School of Medicine, Yokohama, Japan
[2]Laboratory for Bone and Joint Diseases, SNP Research Center, RIKEN, Tokyo, Japan
[3]Department of Orthopaedic Surgery, Nagoya University School of Medicine, Nagoya, Japan
[4]Department of Pediatric Orthopedics, Shizuoka Children's Hospital, Shizuoka, Japan
[5]Division of Clinical Genetics and Cytogenetics, Shizuoka Children's Hospital, Shizuoka, Japan
[6]Department of Paediatrics, Koshigaya Hospital, Dokkyo University School of Medicine, Koshigaya, Japan
[7]Department of Medical Genetics, Kitasato University Graduate School of Medical Sciences, Sagamihara, Japan
[8]Department of Surgical Pathology, Faculty of Medicine, Teikyo University, Tokyo, Japan
[9]Department of Pediatrics, Sapporo Medical University School of Medicine, Sapporo, Japan

Received 29 August 2006; Accepted 21 November 2006

FBN2, *FBN1*, *TGFBR1*, and *TGFBR2* were analyzed by direct sequencing in 15 probands with suspected congenital contractural arachnodactyly (CCA). A total of four novel *FBN2* mutations were found in four probands (27%, 4/15), but remaining the 11 did not show any abnormality in either of the genes. This study indicated that *FBN2* mutations were major abnormality in CCA, and *TGFBR* and *FBN1* defects may not be responsible for the disorder. *FBN2* mutations were only found at introns 30, 31, and 35 in this study. Thus analysis of a mutational hotspot from exons 22 to 36 (a middle part) of *FBN2* should be prioritized in CCA as previously suggested. © 2007 Wiley-Liss, Inc.

Key words: *FBN2*; *FBN1*; *TGFBR1*; *TGFBR2*; congenital contractural arachnodactyly (Beals syndrome)

How to cite this article: Nishimura A, Sakai H, Ikegawa S, Kitoh H, Haga N, Ishikiriyama S, Nagai T, Takada F, Ohata T, Tanaka F, Kamasaki H, Saitsu H, Mizuguchi T, Matsumoto N. 2007. *FBN2*, *FBN1*, *TGFBR1*, and *TGFBR2* analyses in congenital contractural arachnodactyly. Am J Med Genet Part A 143A:694–698.

INTRODUCTION

Congenital contractural arachnodactyly (CCA, OMIM #121050), also known as Beals syndrome, is characterized by skeletal features including arachnodactyly, dolichostenomelia, scoliosis and pectus deformity similar to those found in Marfan syndrome (MFS), but is not usually associated with cardiovascular or ocular features. CCA also shows joint contractures and a crumpled ear deformity. It is often difficult to differentiate between the two syndromes [Viljoen, 1994; Pyeritz, 2000; Gupta et al., 2002, 2004]. Since the first description of *FBN2* abnormalities in CCA, only 22 mutations, to our knowledge, were reported in the literature [Putnam et al., 1995, 1997; Wang et al., 1996; Maslen et al., 1997; Babcock et al., 1998; Park et al., 1998; Belleh et al., 2000; Gupta et al., 2002, 2004] (see also the human gene mutation database: http://www.hgmd.cf.ac.uk/ac/gene.php?gene=FBN2). All *FBN2* mutations clustered in exons 24–33, being analogous to *FBN1* mutations in exons 24–32 identified in neonatal MFS [Tiecke et al., 2001].

Dysregulation of TGFβ signaling is now considered as an important pathogenesis of MFS and MFS-related disorders. Mice with manipulated *Fbn1* showed abnormal TGFβ signaling in affected tissues

Grant sponsor: SORST from Japan Science and Technology Agency (JST); Grant sponsor: Research Promotion Fund from Yokohama Foundation for Advancement of Medical Science; Grant sponsor: Research Promotion Fund from Takeda Science Foundation; Grant sponsor: Research Fund from Uehara Memorial Foundation; Grant sponsor: Sakakibara Memorial Research Grant from the Japan Research Promotion Society for Cardiovascular Diseases.

*Correspondence to: Naomichi Matsumoto, M.D., Ph.D., Department of Human Genetics, Yokohama City University Graduate School of Medicine, Fukuura 3-9, Kanazawa-ku, Yokohama 236-0004, Japan.
E-mail: naomat@yokohama-cu.ac.jp

DOI 10.1002/ajmg.a.31639

[Pereira et al., 1997, 1999; Judge et al., 2004] and mutations of *TGRBR2* and *TGFBR1* have been found in MFS and MFS-related disorders including Loeys–Dietz syndrome (LDS) and familial thoracic aortic aneurysm and dissection (TAAD) in human [Mizuguchi et al., 2004; Loeys et al., 2005; Pannu et al., 2005; Matyas et al., 2006; Singh et al., 2006]. However TGFβ signaling was not investigated in CCA.

In this study, *FBN2*, *FBN1*, *TGFBR1*, and *TGFBR2* were systematically analyzed in a total of 15 CCA patients. Genetic and clinical profiles will be presented.

MATERIALS AND METHODS

Subjects

Patients with CCA or suspected CCA, mostly presenting with joint contractures, marfanoid skeletal features, and ear deformity were recruited for this study. Their detailed clinical features are given in Table I. Among 17 patients including a family with 3 affected, 12 were reasonably evaluated. After written informed consent, genomic DNA of peripheral blood leukocytes was isolated using DNA isolation systems [Quick Gene-800 (Fujifilm, Tokyo, Japan) and/or NA-3000 (Kurabo, Osaka, Japan)]. Ethical approval for this study was obtained from the Committee for Ethical Issues at Yokohama City University School of Medicine.

Sequence Analysis

FBN2, *TGFBR1*, and *TGFBR2* were analyzed in all probands. *FBN1* was lastly analyzed when none of the genes showed abnormality except for one patient (BS9) whose DNA was used up. Exons 22–35 of *FBN2* supposed to cover mutation hotspots were initially screened. If no mutation was found in the hotspots, remaining exons were analyzed. Primer sequences were described elsewhere [Sakai et al., 2006]. Coding exons of *FBN2* (65 exons), *FBN1* (65 exons), *TGFBR1* (9 exons), and *TGFBR2* (7 exons) and their flanking intronic regions were amplified by PCR. PCR products were purified with ExoSAP-IT (USB, Cleveland, OH) and sequenced by a standard protocol using BigDye terminator (Applied Biosystems, Foster City, CA) on an ABI PRISM 3100 Genetic analyzer (Applied Biosystems). Nucleotide changes were confirmed using the SeqScape software ver. 2.5 (Applied Biosystems). If nucleotide substitutions were identified in patients whose parental samples were unavailable, at least 100 normal controls were additionally screened to confirm whether they were polymorphisms or not.

Computational Analysis

Splice site finder (http://www.genet.sickkids.on.ca/~ali/splicesitefinder.html) and ESEfinder (http://rulai.cshl.edu/tools/ESE/) were used for characterization of splice-site-related mutations. At least 30 bp sequences from an exon–intron border and corresponding exonic sequences were analyzed. A wild-type and mutated alleles were compared.

RESULTS AND DISCUSSION

A total of four novel *FBN2* mutations were found in four of 15 CCA probands (27%): IVS30-24A > C, IVS30-5T > G, IVS35 + 1G > T, and IVS31 + 1G > A (Table I). Two of them (IVS30-5T > G and IVS31 + 1G > A) were confirmed to be de novo and one (IVS30-24A > C) was shared by three affected members [dizygotic twin (BS2b and BS2c) and their mother (BS2a)] in one family with a healthy father without the mutation. No mutations were found in *TGFBR1*, *TGFBR2*, or *FBN1*. Polymorphisms were listed in Table II, which were registered in the SNP database (http://www.ncbi.nlm.nih.gov/entrez/query.fcgi?CMD=DisplayFiltered&DB=snp) or observed among 18 normal controls. *FBN2* mutation detection ratios in CCA patients ranged from 18% to 77% [Putnam et al., 1995; Park et al., 1998; Gupta et al., 2002]. This variability could be explained by different techniques, that is, single stranded conformational polymorphism analysis (SSCP) (18%) and SSCP followed by complete sequencing of partial cDNA (78%). In our study, the rate was low regardless of complete sequencing analysis of entire exons including exon–intron borders. This could be partly due to sample bias as each patient was diagnosed with CCA by each clinician. It was noted that all probands with a positive mutation showed joint contractures, marfanoid skeletal features, and ear deformity. *FBN2* analysis is warranted for such full spectrum of CCA phenotypes.

The four mutations we found occurred only at introns 30, 31, and 35 (in the middle of *FBN2*) regardless of complete sequencing of all 65 exons. Thus analysis of mutation hotspots (exons 24–34) is justified as previously suggested [Park et al., 1998]. IVS35 + 1G > T is the most 3′-side mutation ever found. Thus we recommend primary screening of *FBN2* exons 22–36 for CCA.

All *FBN2* mutations found are located at or close to splicing donor or acceptor sites. Splice site finder program demonstrates that IVS30-24A > C and IVS30-5T > G abolish original acceptor sites and the latter creates a new donor site. IVS31 + 1G > A and IVS35 + 1G > T abolish original donor sites (data not shown). Similarly in ESEfinder analysis, IVS30-24A > C creates a new SRp40 site, IVS30-5T > G abolishes an original SRp40 site, IVS31 + 1G > A abolishes original SF2/ASF and SRp40 site to an SRp55 site, and IVS35 + 1G > T abolishes original SF2/ASF and SRp40 sites. Furthermore IVS30-5T > G

TABLE I. Genetic and Clinical Information of Patients

Genetic and clinical information	BS1	BS2a	BS2b	BS2c	BS3	BS4	BS5	BS6	BS7	BS8	BS9	BS10	BS11	BS12a	BS14	BS15	BS16
Mutation																	
FBN2	Normal	IVS30-24A > C	IVS30-24A > C	IVS30-24A > C	Normal	Normal	IVS30-5T > G	Normal	Normal	IVS35 + 1G > T	Normal	IVS31 + 1G > A	Normal	Normal	Normal	Normal	Normal
FBN1	Normal				Normal	Normal		Normal	Normal		Unknown		Normal	Normal	Normal	Normal	Normal
TGFBR1	Normal	Normal	–	–	Normal	Normal	Normal	Normal	Normal	Normal	Normal	Normal	Normal	Normal	Normal	Normal	Normal
TGFBR2	Normal	Normal	–	–	Normal	Normal	Normal	Normal	Normal	Normal	Normal	Normal	Normal	Normal	Normal	Normal	Normal
Nature		Familial	Familial	Familial			De novo			Not confirmed		De novo					
Sex	Female	Female	Female	Male	Female	Male	Female	Male	Male	Female	Female	Female	Female	Male	Female	Female	Male
Age		18 y	17 m	18 m	18 y	0				4 y		13 y	0	4 y	24 y	5 y	7 y
Height (cm)		161	85	84	156					114		104	50		133	98	128
Weight (kg)		75	9.5	12	52					17		14	4.3		33	13	15
Age at diagnosis (year)			0	0	11					10 m		10	0	1	0	4	7
Family history		+	+	+	–	–				Unknown		–	–	–	+	–	–
Cranial abnormality		–	Dolichocephaly	–	–					–		Open anterior fontanelle	+	–	–	–	–
Eye abnormality		–	–	–	–	Small palpebral fissures				–		Amblyopia	–	–	–	–	Hyperopia
Abnormal ears		+	+	+	+	+				+		+	–	+	–	–	+
High arched palate		+	+	+	–	+				–		–	–	–	+	–	–
Micrognathia		+	+	+	–	+				–		–		–	+	–	
Congenital contractures												+					
Shoulder		–	–	–	+	–				–		+	–	–	–	–	–
Elbow		–	+	–	+	+				+		+	–	–	–	–	+
Knee		–	–	–	+	+				+		+	–	–	–	–	+
Hip		–	–	–	–	–				+		+	+	–	–	–	+
Finger		+	+	–	+	+				+		+	+	+	+	+	+
Toe		–	+	–	+	+				–		+	–	–	+	–	+
Wrist		–	–	–	–	–				–		+	–	–	+	–	+
Scoliosis		+	–	–	+	+				+		+	+	–	–	–	+
Pectus deformity		–	–	–	–	–				–		+	–	–	–	–	–
Arachnodactyly		–	+	–	+	+				+		+	+	+	+	–	+
Bowed long bone		–	–	–	–	–				–		+	–	–	–	–	–
Club foot		–	–	–	–	–				–		–	+	–	–	–	+
Hypotonia		–	–	–	–					–		–	–	–	–	–	+
Improvement of contractures		–	+	–	+					–		–	–	+		Operated	–
Cardiovascular abnormality		–	–	–	–	PDA				–		–	–	PS, AS	Dextrocardia	PDA	–
Mental retardation		+	–	–	–	+				–		–		–	–	–	+
Others			Rocker bottom foot	rocker bottom foot		Auditory defect Micropenis Lt. multicystic kidney Vesical diverticulum Rt. hydronephrosis						Rt. anotia			Cleft palate	Conduction deafness	Hydrocephalus

PS, pulmonary stenosis; AS, aortic stenosis.

American Journal of Medical Genetics Part A: DOI 10.1002/ajmg.a

TABLE II. Polymorphisms Found in This Study

Gene	Exon	Polymorphism	SNP ID	Allele frequency in normal control
FBN2	1	244G > A (V82M)		Found in a healthy parent
FBN2	22	IVS22 + 23G > T	rs255690	
FBN2	23	2893G > A (V965I)	rs154001	
FBN2	27	3518C > G (T1173S)		Found in a healthy parent
FBN2	44	IVS44-9C > T	rs27713	
FBN2	46	5823T > C (H1941H)	rs11955288	
FBN2	48	IVS48 + 24G > A	rs28763934	
FBN2	50	IVS50-26T > C	ss16338560	
FBN2	51	IVS51 + 15A > G		7/36
FBN2	54	IVS54 + 17G > A	rs2042327	
FBN2	55	6931A > G (M2311V)	rs32209	
FBN2	55	IVS55-5T > C	rs28763927	
FBN2	57	7200T > C (S2400S)	rs190450	
FBN2	61	7739C > T (S2580L)	rs2291628	
TGFBR1	7	IVS7 + 24G > A	rs334354	
TGFBR2	5′-UTR	5′-UTR-128C > G	rs2306856	
TGFBR2	2	IVS2 + 7A > G	rs1155705	
TGFBR2	3	IVS3-4T > A	rs11466512	
TGFBR2	4	1242C > T (T414T)	rs2228048	

and IVS31 + 1G > A were do novo changes and IVS30-24A > C and IVS31 + 1G > A were not found in at least 100 normal controls. Thus all mutations are likely to be pathogenic.

TGFBR mutations were not found in our CCA series, but found in MFS, LDS, TAAD, and Shprintzen–Goldberg craniosynostosis syndrome (SGS) [Mizuguchi et al., 2004; Loeys et al., 2005; Pannu et al., 2005; Kosaki et al., 2006; Matyas et al., 2006; Singh et al., 2006]. Dysregulation of TGFβ signaling is now considered as the core pathogenesis of MFS and MFS-related disorders. Fibrillin 2 and fibrillin 1 are the major structural components of extracellular microfibrils [Handford et al., 2000]. We expected that a subset of CCA patients may have *TGFBR* mutations, but they did not. *Fbn2* homozygous knockout mice presented with contractures of forelimbs and stiff large joints of hindlimbs which are found in human CCA and also unexpected syndactyly [Arteaga-Solis et al., 2001]. As functional interaction of Fbn2 and Bmp-7 was suggested by double heterozygous Fbn2/Bmp-7 mice which showed combined the patterning defects of each nullyzygous mice, Bmp signaling instead of Tgfβ signaling may be functionally correlated with Fbn2 [Arteaga-Solis et al., 2001].

In conclusion, we found four novel *FBN2* mutations in 4 of 15 CCA patients (27%), but none of other did show *TGFBR1*, *TGFBR2*, *FBN2*, or *FBN1* abnormality, being genetically unexplained. It would be interesting to investigate BMP signaling in CCA patients.

This work was supported by SORST from Japan Science and Technology Agency (JST) for N. M., Research Promotion Fund from Yokohama Foundation for Advancement of Medical Science for N. M., Research Promotion Fund from Takeda Science Foundation for N. M., Research Fund from Uehara Memorial Foundation for N. M., and a Sakakibara Memorial Research Grant from the Japan Research Promotion Society for Cardiovascular Diseases for T. M.

REFERENCES

Arteaga-Solis E, Gayraud B, Lee SY, Shum L, Sakai L, Ramirez F. 2001. Regulation of limb patterning by extracellular microfibrils. J Cell Biol 154:275–281.

Babcock D, Gasner C, Francke U, Maslen C. 1998. A single mutation that results in an Asp to His substitution and partial exon skipping in a family with congenital contractural arachnodactyly. Hum Genet 103:22–28.

Belleh S, Zhou G, Wang M, Der Kaloustian VM, Pagon RA, Godfrey M. 2000. Two novel fibrillin-2 mutations in congenital contractural arachnodactyly. Am J Med Genet 92:7–12.

Gupta PA, Putnam EA, Carmical SG, Kaitila I, Steinmann B, Child A, Danesino C, Metcalfe K, Berry SA, Chen E, Delorme CV, Thong MK, Ades LC, Milewicz DM. 2002. Ten novel FBN2 mutations in congenital contractural arachnodactyly: Delineation of the molecular pathogenesis and clinical phenotype. Hum Mutat 19:39–48.

Gupta PA, Wallis DD, Chin TO, Northrup H, Tran-Fadulu VT, Towbin JA, Milewicz DM. 2004. FBN2 mutation associated with manifestations of Marfan syndrome and congenital contractural arachnodactyly. J Med Genet 41:e56.

Handford PA, Downing AK, Reinhardt DP, Sakai LY. 2000. Fibrillin: From domain structure to supramolecular assembly. Matrix Biol 19:457–470.

Judge DP, Biery NJ, Keene DR, Geubtner J, Myers L, Huso DL, Sakai LY, Dietz HC. 2004. Evidence for a critical contribution of haploinsufficiency in the complex pathogenesis of Marfan syndrome. J Clin Invest 114:172–181.

Kosaki K, Takahashi D, Udaka T, Kosaki R, Matsumoto M, Ibe S, Isobe T, Tanaka Y, Takahashi T. 2006. Molecular pathology of Shprintzen-Goldberg syndrome. Am J Med Genet Part A 140A:104–108; Author reply 109–110.

Loeys BL, Chen J, Neptune ER, Judge DP, Podowski M, Holm T, Meyers J, Leitch CC, Katsanis N, Sharifi N, Xu FL, Myers LA, Spevak PJ, Cameron DE, De Backer J, Hellemans J, Chen Y, Davis EC, Webb CL, Kress W, Coucke P, Rifkin DB, De Paepe AM, Dietz HC. 2005. A syndrome of altered cardiovascular, craniofacial, neurocognitive and skeletal development caused by mutations in TGFBR1 or TGFBR2. Nat Genet 37:275–281.